

# Oxidation Behavior of a Pd<sub>43</sub>Cu<sub>27</sub>Ni<sub>10</sub>P<sub>20</sub> Bulk Metallic Glass and Foam in Dry Air

W. KAI, I.F. REN, B. BARNARD, P.K. LIAW, M.D. DEMETRIOU, and W.L. JOHNSON

The oxidation behavior of both Pd<sub>43</sub>Cu<sub>27</sub>Ni<sub>10</sub>P<sub>20</sub> bulk metallic glass (Pd4-BMG) and its amorphous foam containing 45 pct porosity (Pd4-AF) was investigated over the temperature range of 343 K (70 °C) to 623 K (350 °C) in dry air. The results showed that virtually no oxidation occurred in the Pd4-BMG at  $T < 523$  K (250 °C), revealing the alloy's favorable oxidation resistance in this temperature range. In addition, the oxidation kinetics at  $T \geq 523$  K (250 °C) followed a parabolic-rate law, and the parabolic-rate constants ( $k_p$  values) generally increased with temperature. It was found that the oxidation  $k_p$  values of the Pd4-AF are slightly lower than those of the Pd4-BMG, indicating that the porous structure contributes to improving the overall oxidation resistance. The scale formed on the alloys was composed exclusively of CuO at  $T \geq 548$  K (275 °C), whose thickness gradually increased with increasing temperature. In addition, the amorphous structure remained unchanged at  $T \leq 548$  K (275 °C), while a triplex-phase structure developed after the oxidation at higher temperatures, consisting of Pd<sub>2</sub>Ni<sub>2</sub>P, Cu<sub>3</sub>P, and Pd<sub>3</sub>P.

DOI: 10.1007/s11661-010-0231-5

© The Minerals, Metals & Materials Society and ASM International 2010

## I. INTRODUCTION

PRECIOUS-METAL-BASED amorphous alloys, such as Pd<sub>40</sub>Ni<sub>40</sub>P<sub>20</sub> (Pd3-BMG), have been developed since the past decades.<sup>[1,2]</sup> One of the important features for this amorphous alloy was its relatively low glass-transition temperature ( $T_g \approx 580$  K (307 °C)) and good thermal stability ( $T_x \approx 660$  K (387 °C)), which provided a large supercooled liquid region ( $\Delta T_x = T_x - T_g$ ) of 80 K (80 °C). It was reported that, upon relaxation at a temperature near  $T_g$ , this ternary alloy could be easily deformed with an excellent superplasticity of 1260 pct, which made it possible to form complex shapes for industrial applications.<sup>[3]</sup>

Most recently, the quaternary version of this family, the Pd-Cu-Ni-P glassy alloy, has been extensively studied, and the results indicated that the critical cooling rates to retain the glassy structure were significantly lower than those of the ternary alloy.<sup>[4-6]</sup> In addition, it was also found that the quaternary amorphous alloy containing certain amounts of porosity (*i.e.*, metallic glass foam) exhibited interesting mechanical properties.

For example, in the porosity range of 36 to 70 pct, Pd<sub>42.5</sub>Cu<sub>30</sub>Ni<sub>7.5</sub>P<sub>20</sub> and Pd<sub>43</sub>Cu<sub>27</sub>Ni<sub>10</sub>P<sub>20</sub> foams exhibited strengths in the range of 100 to 600 MPa, elastic moduli in the range of 6 to 32 MPa, and plastic deformation up to 20 to 30 pct strain.<sup>[6-8]</sup> Nevertheless, the use of Pd4-BMG and its foam in practical applications at higher temperatures requires knowledge of its degradation behavior during oxidation. Thus, it is of interest to investigate the oxidation behavior of the Pd4-BMG and its foamy material in this study.

## II. EXPERIMENTAL

The starting materials contained high purity of elemental turnings (at least 99.99 vol. pct pure). A Pd<sub>43</sub>Cu<sub>27</sub>Ni<sub>10</sub>P<sub>20</sub> amorphous disk 12 mm in diameter and 4 mm in length (Pd4-BMG) was prepared by injection casting. Another porous Pd<sub>43</sub>Cu<sub>27</sub>Ni<sub>10</sub>P<sub>20</sub> disk containing about 45 pct porosity (Pd4-AF), having the same size of Pd4-BMG, was prepared by thermoplastic expansion of entrained gas bubbles.<sup>[9]</sup> The average composition of the two samples done by the X-ray wavelength-dispersive spectroscopy is 42.1 pct Pd, 25.9 pct Cu, 10.8 pct Ni, and 21.2 pct P (hereinafter in atomic percent unless otherwise stated). Both bulk and foam samples (2 × 2 × 1 mm) for oxidation tests were directly sheared from the amorphous disks, ground, and polished down to 1200 SiC abrasive papers, cleaned with acetone, and immediately dried before the tests. The actual area ( $A_{\text{true}}$ ) of the porous samples was approximately estimated from the measured area ( $A_o$ ) by the equation of

$$A_{\text{true}} = A_o \times \left[ 1 + \left( \frac{\text{porosity pct}}{100} \right)^{2/3} \right] \quad [1]$$

W. KAI, Professor, and I.F. REN, Graduate Student, are with the Institute of Materials Engineering, National Taiwan Ocean University, Keelung, 20224, Taiwan, Republic of China. Contact e-mail: wkai@mail.ntou.edu.tw B. BARNARD, Graduate Student, and P.K. LIAW, Professor, are with the Department of Materials Science and Engineering, University of Tennessee, Knoxville, TN 37996. M.D. DEMETRIOU, Senior Research Fellow, and W.L. JOHNSON, Professor, are with the Department of Materials Science, Keck Laboratory, California Institute of Technology, Pasadena, CA 91125.

This article is based on a presentation given in the symposium "Bulk Metallic Glasses VI," which occurred during the TMS Annual Meeting, February 15–19, 2009, in San Francisco, CA, under the auspices of TMS, the TMS Structural Materials Division, TMS/ASM: Mechanical Behavior of Materials Committee.

Article published online May 13, 2010

Oxidation tests of the alloy were performed by means of the thermogravimetric analyzer (TGA) in dry air (>99.999 vol. pct pure). The net flow rate of air was kept constant at 40 cm<sup>3</sup>/min throughout each test. The heating and cooling rates of TGA were set to 10 K/min (10 °C/min). The characterization of the alloys and oxide scales was carried out using X-ray diffraction (XRD), a scanning electron microscope equipped with an energy-dispersive spectrometer (EDS), an electron-probe microanalyzer (EPMA) equipped with a wavelength dispersive spectrometer, and a transmission electron microscope (TEM) equipped with an image analyzer, EDS, and selected-area diffraction (SAD).

### III. RESULTS AND DISCUSSION

#### A. Alloy Constitution and Thermal Analyses

The XRD spectra of the as-cast alloys are shown in Figure 1, revealing that two wide-broadening peaks near  $2\theta = 41.1$  deg and  $71.9$  deg were noted, which further indicated the amorphous structure of the samples. The DSC curves of the alloys shown in Figure 2 reveal that the  $T_g$  and  $T_x$  temperatures are 583.2 K (310.2 °C) and 660.5 K (387.5 °C) and 582.3 K (309.3 °C) and 659.1 K (386.1 °C) for the Pd4-BMG and Pd4-AF, respectively. According to the results of XRD and DSC, it is clear that the porosity did not make any significant difference for the two amorphous samples, and the oxidation tests were set from room temperature to 623 K (350 °C).

#### B. Oxidation Kinetics

The oxidation-kinetics curves of the Pd4-BMG and Pd4-AF over the temperature range of 523 K (250 °C) to 623 K (350 °C) are shown as the parabolic plot in Figure 3. In general, the oxidation kinetics followed a two-stage parabolic-rate law for both glassy alloys, indicating that diffusion is the rate-controlling step during oxidation. The observed two-stage kinetics

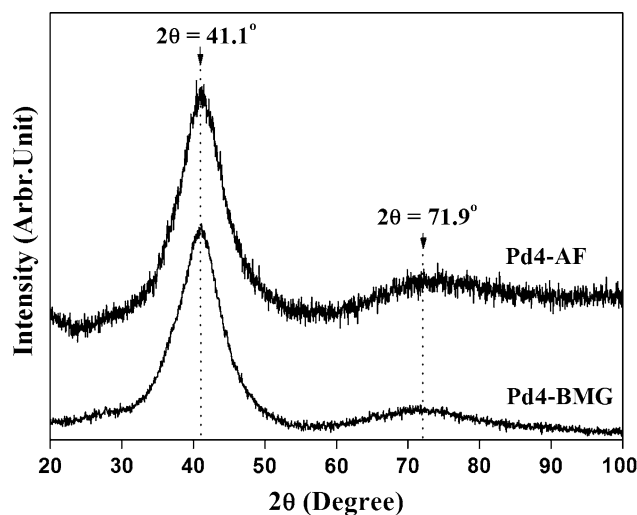


Fig. 1—XRD spectra of the Pd4-based glassy alloys.

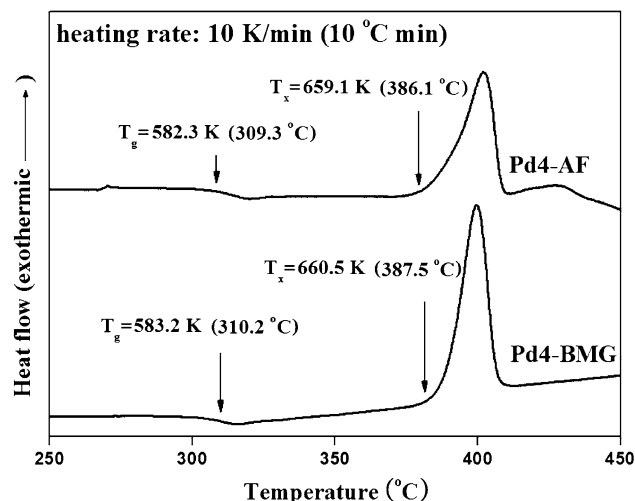


Fig. 2—DSC curves of the Pd4-BMG and Pd4-AF obtained at a heating rate of 10 K/min (10 °C/min).

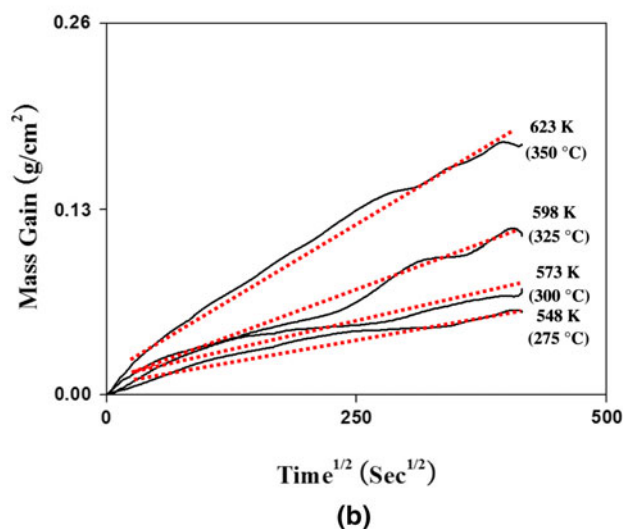
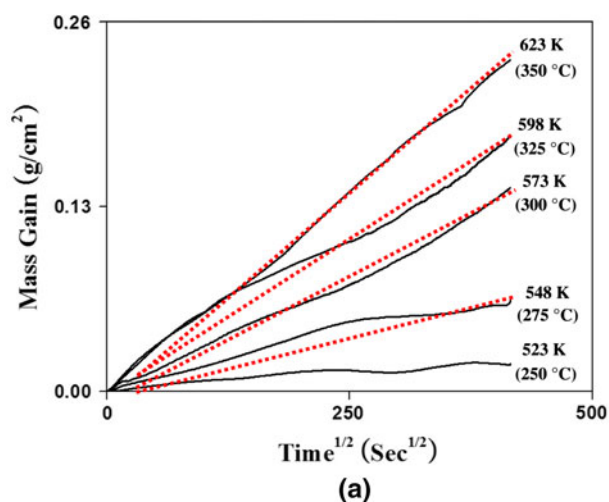


Fig. 3—Parabolic plots of the mass-gain data for the (a) Pd4-BMG and (b) Pd4-AF.

consisted of an initial slow-growth nucleation of scales (up to about 1800 seconds) and a second steady-state stage of oxidation (the fitting was shown by the dashed line). In addition, the steady-state parabolic-rate constants can be calculated as an equation between the mass-gain data and the exposure time ( $t$ ):

$$(\Delta m/A)^2 = k_p t + C \tag{2}$$

where  $\Delta m$ ,  $A$ ,  $k_p$ , and  $C$  are the mass-gain data, sample area, parabolic-rate constant, and integration constant, respectively. The mass-gain datum of the Pd4-BMG at 523 K (250 °C) was very small, only about  $1.9 \times 10^{-5}$  g/cm<sup>2</sup> after a 48-hour exposure. Furthermore, attempts to oxidize three amorphous samples at 473 K (200 °C) or lower for 48 hours were not successful, since the overall mass gain was insufficient to be detected by TGA-detection limits. This observation further implies that nearly no oxidation occurred for the samples at temperatures below 523 K (250 °C). Therefore, the

results and discussion of this study will focus primarily on the data obtained at 548 K (275 °C) or higher temperatures. In addition, the oxidation-rate constants ( $k_p$  values) of the two samples at steady stage are shown in Table I. The  $k_p$  values of pure Cu obtained in the same atmosphere are also presented in the same table for comparison. From the data in the table, it is evident that the  $k_p$  values of the Pd4-AF are slightly lower than those of the Pd4-BMG, while both samples exhibited a better oxidation resistance with respect to pure Cu. The main reason for the lower oxidation rates of the amorphous alloys, relative to pure Cu, is due presumably to the formation of slower-growth scales, as discussed later.

C. Scale Constitution and Phases

Cross-sectional backscattered-electron-image (BEI) micrographs and the corresponding XRD analyses of the scales formed on the Pd4-BMG and Pd4-AF

Table I. Parabolic-Rate Constants of the Pd4-Based Glassy Alloys and Pure Cu in Dry Air ( $k_p$ , g<sup>2</sup>/cm<sup>4</sup>/s)

Material	Temperature				
	523 K (250 °C)	548 K (275 °C)	573 K (300 °C)	598 K (325 °C)	623 K (350 °C)
Pd4-BMG	$4.8 \times 10^{-16}$	$3.7 \times 10^{-15}$	$8.6 \times 10^{-14}$	$1.1 \times 10^{-13}$	$3.2 \times 10^{-13}$
Pd4-AF	—	$3.2 \times 10^{-15}$	$1.4 \times 10^{-14}$	$8.1 \times 10^{-14}$	$1.9 \times 10^{-13}$
Pure Cu	—	—	$5.3 \times 10^{-13}$	—	$2.3 \times 10^{-12}$

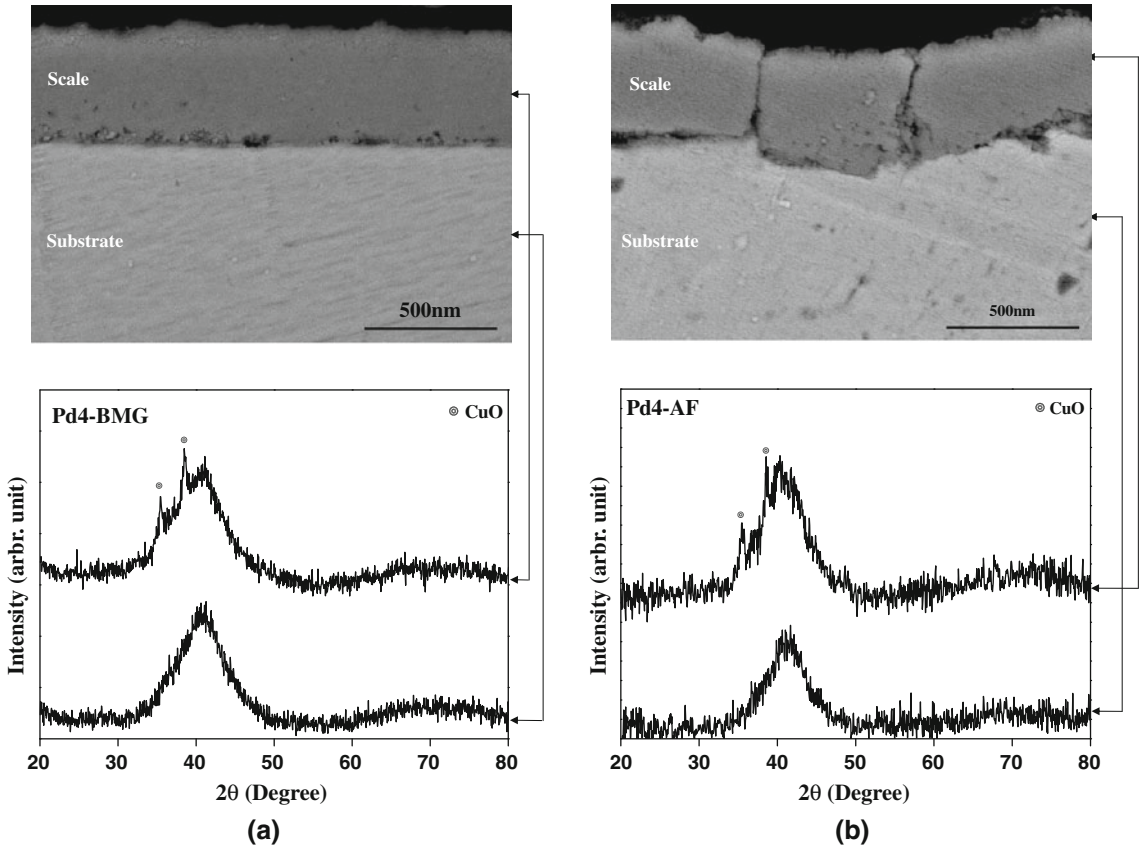


Fig. 4—BEI micrographs and corresponding XRD spectra of the (a) Pd4-BMG and (b) Pd4-AF after oxidation for 48 h at 548 K (275 °C).



oxidized for 48 hours at 548 K (275 °C) are shown in Figure 4. A thin single-layer scale formed on the two alloys with an average thickness of the bulk and foamy samples is about  $448 \pm 21$  nm and  $365 \pm 31$  nm, respectively. The observed thin-scale thickness is in good agreement with the slow kinetics for the amorphous alloys. Based on XRD analyses, the scale formed at this temperature was exclusively CuO, while the substrate retained the amorphous nature. A BEI micrograph and the corresponding XRD analyses of cross-sectional scales formed on the Pd4-BMG oxidized 48 hours at 573 K (300 °C) are shown in Figures 5(a) and (b). A single scale layer is also observed, the thickness of which is around  $633 \pm 78$  nm. XRD analyses revealed that the scale consisted exclusively of CuO layer, which is intermixed with three crystalline phases of mostly Pd<sub>3</sub>P and minor amounts of Pd<sub>2</sub>Ni<sub>2</sub>P and Cu<sub>3</sub>P. The presence of three crystalline phases may be due to the thin-scale nature, which allows the penetration of X-ray down to the substrate. The observed crystalline phases further indicated that the amorphous substrate started to crystallize at this temperature after a 48-hour exposure.

In a literature review article,<sup>[10]</sup> it is reported that a duplex scale of Cu<sub>2</sub>O and CuO is known to always form in the oxidation of pure Cu, although the metastable Cu<sub>1.5</sub>O phase might grow at a temperature below 473 K (200 °C). In addition, the Cu<sub>4</sub>O<sub>3</sub> phase was also observed in a previous study concerning the oxidation of the Cu<sub>60</sub>Hf<sub>25</sub>Ti<sub>15</sub> glassy alloy at 648 K (375 °C) to 793 K (520 °C).<sup>[11]</sup> Thus, one may expect that the growth of duplex or complex copper oxides on top of the Pd4-BMG is kinetically favorable. However, the observed results indicated that an exclusive CuO layer was present, which deserves further verification through TEM. A typical cross-sectional TEM bright-field image, as shown in Figure 5(c), reveals a larger dark oxide particle embedded in the white area. SAD patterns taken from the particle (within the white-circle region in the figure) confirm the existence of CuO. Furthermore, the cross-sectional BEI micrographs of the Pd-based glassy alloys oxidized at 598 K (325 °C) to 623 K (350 °C) for 48 hours were further exemplified in Figure 6. An exclusive CuO layer was also detected on the two samples, and their thickness (~800 nm to 1 μm) was much greater than that at lower temperatures. Note that the substrate revealed at least two different images; the bright phase analyzed by EDS revealed 66.6 pct Pd, 24.4 pct P, and 9 pct Cu, which was close to the Pd<sub>3</sub>P dissolved minor amounts of Cu, while the gray phase contained about 37.1 pct Pd, 29.9 pct Cu, 21.2 pct P, and 11.8 pct Ni, which might be close to the intermixed Pd<sub>2</sub>Ni<sub>2</sub>P and Cu<sub>3</sub>P.

As also described previously,<sup>[11]</sup> Cu<sub>2</sub>O has large deviations from the stoichiometry, and its nonstoichiometric value (the *x* value in Cu<sub>2-*x*</sub>O) is around 0.002 at 1298 K (1025 °C) and 0.1 atm O<sub>2</sub>. On the other hand, Tretyakov *et al.*<sup>[12]</sup> reported that CuO<sub>1-*y*</sub> has very small deviations from stoichiometry, and its *y* value is around  $1.1 \times 10^{-19}$  at 1073 K (800 °C) and 0.21 atm O<sub>2</sub>. In other words, the defect concentration in the CuO is much lower than that in the Cu<sub>2</sub>O. Thus, the absence of the highly defective Cu<sub>2</sub>O in the Pd4-based glassy

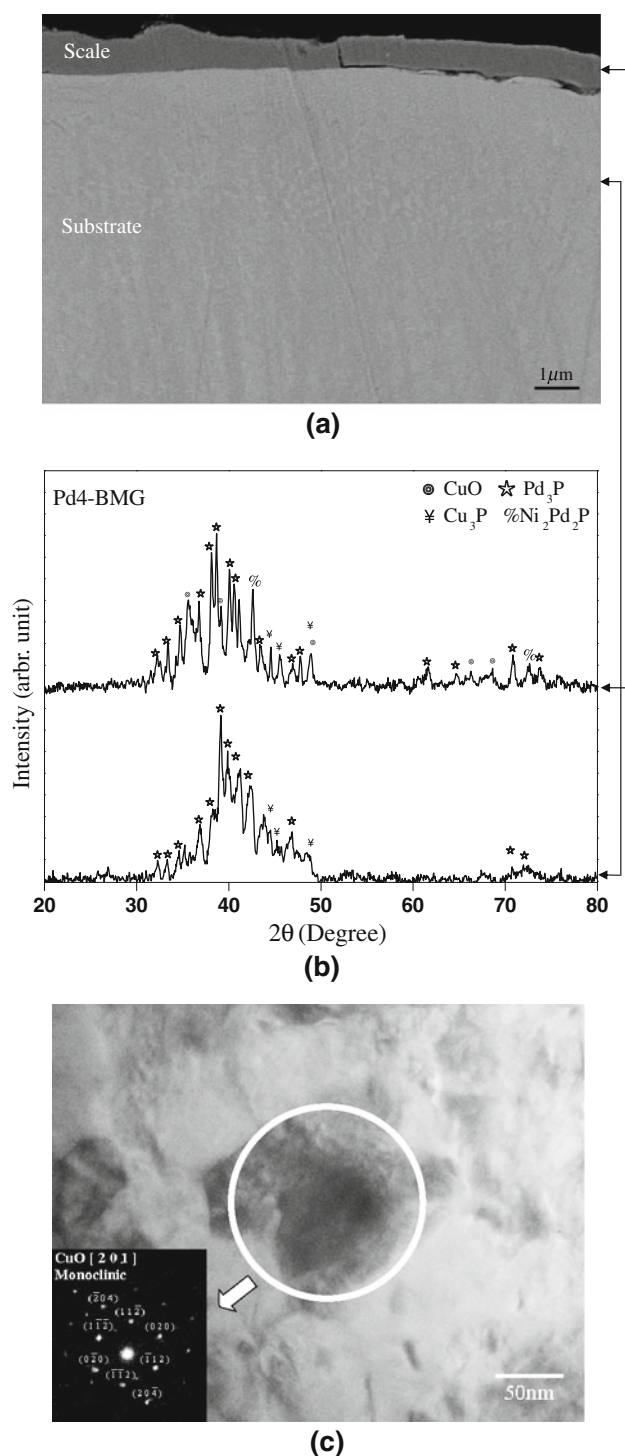


Fig. 5—(a) BEI micrographs and (b) corresponding XRD spectra of the Pd4-BMG after oxidation for 48 h at 573 K (300 °C). (c) TEM bright-field images with inserted SAD patterns for the CuO particle in the scales.

samples is responsible for the slow-scaling rate with respect to the oxidation of pure Cu. In addition, an interesting aspect to discuss is the possibility of forming other oxides in the alloy, since the glassy alloy contains high amounts of other alloying elements (73 pct). Based on the Gibbs-free energies of formation of the stable

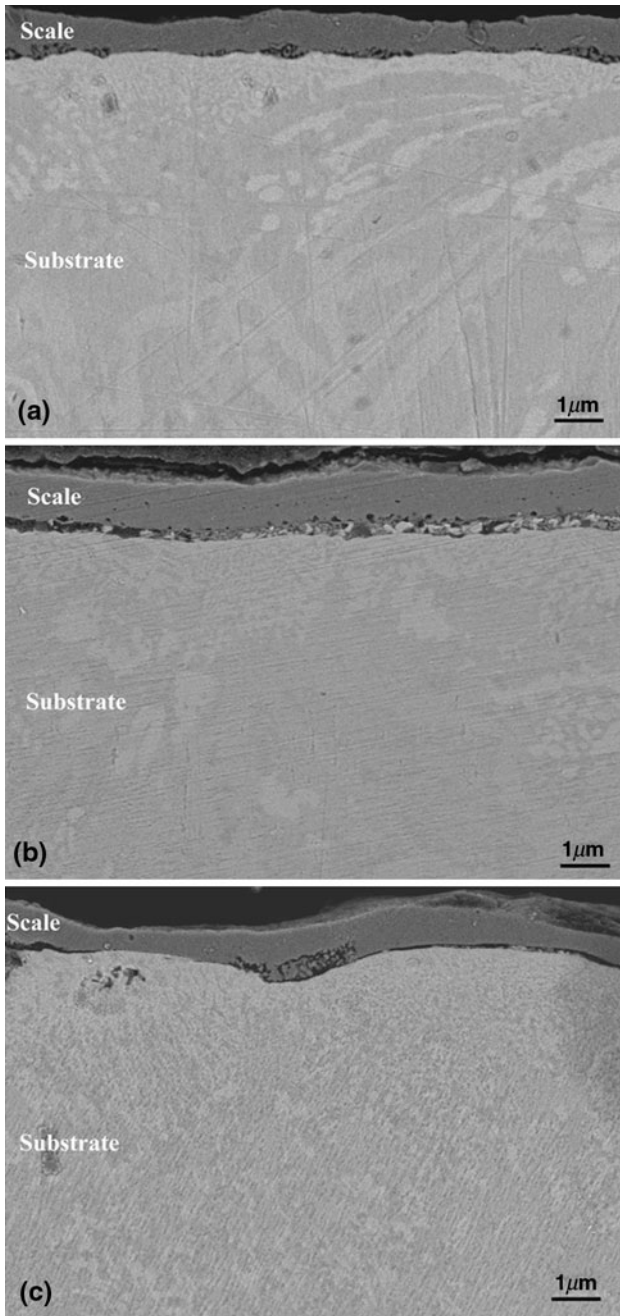


Fig. 6—BEI micrographs of the Pd4-BMG oxidized for 48 h (a) at 598 K (325 °C) and (b) at 623 K (350 °C) and (c) the Pd4-AF oxidized for 48 h at 598 K (325 °C).

oxides, as shown in Table II, the free energies of  $P_2O_5$  and NiO are more negative than those of  $CuO/Cu_2O$ . One would expect that the formation of either  $P_2O_5$ , NiO, or both could be thermodynamically favorable, because their dissociation partial pressures are much lower than the local oxygen pressure between copper oxides and the substrate. However, none of them was detected by XRD, EPMA, and TEM analyses. Very likely, the scaling rate of CuO is much faster than that of other oxides, so that the formation of  $P_2O_5$  or NiO becomes kinetically unfavorable.

Table II. The Standard Gibbs-Free Energies of Formation ( $\Delta G_f^\circ$ ) of Some Oxides at 523 K (250 °C) to 623 K (350 °C) (kJ/mol  $O_2$ )

$\Delta G_f^\circ$ (kJ/mol $O_2$ )	523 K (250 °C)	573 K (300 °C)	623 K (350 °C)
NiO	−381.6	−372.7	−363.9
PdO	−123.7	−113.2	−102.7
$P_2O_5$	−499.8	−490.5	−481.3
CuO	−215.5	−206.5	−197.7

Another interesting aspect to further discuss is the effect of porosity on the oxidation rate of the amorphous alloy. In general, the higher the porosity, the higher the true area exposed to the oxidized environments, which, in turn, enhances the reaction between the substrate and oxygen, thereby leading to an increase of the oxidation rate. However, the kinetic results in Table I indicate that the reverse situation was realized in the current study. The observation that the porous sample exhibits a better oxidation resistance than the bulk is rather intriguing. One plausible cause could be that the presence of pores (voids) contributes to lengthening the average diffusion path of cations and oxygen through the porous structure as compared to the fully-dense sample, and in turn reduces the possible scaling rate of the foam under the same exposure duration thereby leading to lower  $k_p$  values. Another cause could be attributed to the difference in the overall surface roughness of the two samples, which can result in different catalytic features dictating heterogeneous oxidation. As noted previously, the surfaces of both the bulk and porous samples were polished down to 1200 grit. The cavity regions in the porous surface, however, consist of as-formed rather than polished material, and hence lack the coarser polishing microfeatures that appear in the polished regions of both samples. It is therefore plausible that the near-perfect roughness within cavities, which is essentially on the order of the atomic-scale features of the glassy nanostructure, effectively constrains heterogeneous oxidation within those regions giving rise to an overall improved oxidation resistance for the porous sample.

#### D. Short-Term Oxidation

In order to understand the relationship between the oxidation and crystallization of the Pd4-BMG, short-term oxidation tests were performed at 573 K (300 °C). Typical XRD analyses of this alloy oxidized at various durations are shown in Figure 7. Clearly, small amounts of CuO were formed on the amorphous substrate after an initial oxidation for 3 hours. In addition, some  $Pd_3P$  could be detected at the same temperature after a 7.5 hour exposure, while minor amounts of  $Cu_3P$  and  $Pd_2Ni_2P$  were observed after a prolonged oxidation for 12 hours. Therefore, the growth of CuO on the Pd4-BMG sample at 573 K (300 °C) was always present at the beginning of oxidation, followed by the crystallization of  $Pd_3P$  and then by the formation of  $Cu_3P$  and  $Pd_2Ni_2P$  at an eventual steady state.

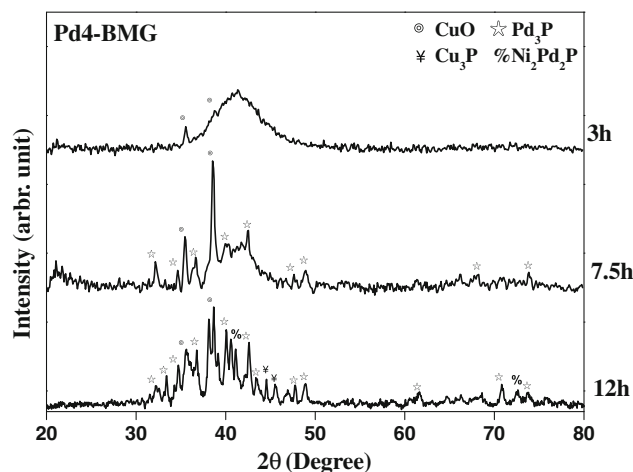


Fig. 7—XRD analyses of the Pd4-BMG after oxidation at 573 K (300 °C) for various durations of time.

#### IV. CONCLUSIONS

The oxidation behavior of bulk and porous (45 pct porosity)  $\text{Pd}_{43}\text{Cu}_{27}\text{Ni}_{10}\text{P}_{20}$  amorphous samples was investigated over the temperature range of 343 K (70 °C) to 623 K (350 °C) in dry air. The following conclusions were drawn.

1. No detectable oxidation was observed at  $T < 523$  K (250 °C), while the oxidation kinetics of the amorphous alloys at  $T \geq 548$  K (275 °C) followed a two-stage parabolic-rate law, indicating that diffusion is the rate-controlling step. The steady-state  $k_p$  values increased with increasing temperature.
2. The scale formed on the amorphous alloys was exclusively CuO, and its amounts increased with increasing temperature.
3. The absence of  $\text{Cu}_2\text{O}$  and other oxides resulted in a better oxidation resistance for the amorphous alloys, as compared to that of pure Cu.
4. The amorphous nature of the substrate remained unchanged after the oxidation for 47 hours at  $T \leq 548$  K (275 °C), while three crystalline phases

of  $\text{Pd}_3\text{P}$ ,  $\text{Cu}_3\text{P}$ , and  $\text{Pd}_2\text{Ni}_2\text{P}$  were detected at higher temperatures. The phase transformation of the amorphous alloys started from the growth of CuO at the beginning of oxidation, followed by the crystallization of  $\text{Pd}_3\text{P}$ , and then by the formation of  $\text{Cu}_3\text{P}$  and  $\text{Pd}_2\text{Ni}_2\text{P}$  at an eventual steady state.

#### ACKNOWLEDGMENTS

The authors are thankful for the financial support by the National Science Council of the Republic of China under Grant No. NSC-96-2218-E-011-001. Special thanks are due to Dr. R.T. Huang, NTOU, for the TEM sample preparation and operation assistance. One of the authors (PKL) is very grateful for the financial support of the National Science Foundation International Materials Institutes (IMI) programs (Grant No. DMR 0231320) with Dr. C. Huber as the program director.

#### REFERENCES

1. H.S. Chen: *Acta Metall.*, 1974, vol. 22, pp. 1505–11.
2. H.W. Kui, A.L. Greer, and D. Turnbull: *Appl. Phys. Lett.*, 1984, vol. 45, pp. 615–16.
3. Y. Kawamura, T. Nakamura, and A. Inoue: *Scripta Mater.*, 1998, vol. 39, pp. 301–06.
4. A. Inoue, A. Kato, T. Zhang, S.G. Kim, and T. Masumoto: *Mater. Trans. JIM*, 1991, vol. 32, pp. 609–16.
5. N. Nishiyama and A. Inoue: *Appl. Phys. Lett.*, 2002, vol. 80, pp. 568–70.
6. T. Wada and A. Inoue: *Mater. Trans.*, 2004, vol. 45, pp. 2761–65.
7. T. Wada, K. Kawamura, N. Nishiyama, and A. Inoue: *Mater. Trans.*, 2005, vol. 46, pp. 2777–80.
8. M.D. Demetriou, J.C. Hanan, C. Veazey, M.D. Michiel, N. Lenoir, E. Üstündag, and W.L. Johnson: *Adv. Mater.*, 2007, vol. 19, pp. 1957–62.
9. M.D. Demetriou, C. Veazey, J. Schroers, J.C. Hanan, and W.L. Johnson: *J. Alloys Compd.*, 2007, vols. 434–435, pp. 92–96.
10. P. Kofstad: *High Temperature Corrosion*, Elsevier Applied Science, New York, NY, 1988, pp. 186–88.
11. W. Kai, H.H. Hsieh, T.H. Ho, R.T. Huang, and Y.L. Lin: *Oxid. Met.*, 2007, vol. 68, pp. 177–92.
12. Y.D. Tretyakov, V.F. Komarov, N.A. Prosvirina, and I.B. Kutsenok: *J. Solid State Chem.*, 1972, vol. 5, pp. 157–67.